Published in final edited form as:
Traffic. 2008 May ; 9(5): 742–754. doi:10.1111/j.1600-0854.2008.00712.x.

ITSN-1 Controls Vesicle Recycling at the Neuromuscular Junction and Functions in Parallel with DAB-1

Wei Wang[1], **Magali Bouhours**[2], **Elena O. Gracheva**[3], **Edward H. Liao**[2], **Keli Xu**[1], **Ameet S. Sengar**[1,4,5], **Xiaofeng Xin**[4,6], **John Roder**[2,4], **Charles Boone**[4,6], **Janet E. Richmond**[3], **Mei Zhen**[2,4], and **Sean E. Egan**[1,4,*]

[1]Program in Developmental and Stem Cell Biology, The Hospital for Sick Children. 101 College Street, TMDT East Tower, Toronto, Ontario M5G 1L7, Canada

[2]Samuel Lunenfeld Research Institute, Mount Sinai Hospital, and Department of Physiology, University of Toronto, Toronto, Ontario M5G 1X5, Canada

[3]Department of Biological Sciences, University of Illinois, Chicago, IL 60607, USA

[4]Department of Molecular Genetics, University of Toronto, Toronto, Ontario, Canada

[5]Neuroscience and Mental Health, The Hospital for Sick Children, 555 University Avenue, Room 5020 McMaster Building, Toronto, Ontario M5G 1X8, Canada

[6]Terrence Donnelly Center for Cellular and Biomolecular Research, 160 College Street, Toronto, Ontario M5S 3E1, Canada

Abstract

Intersectins (Itsn) are conserved EH and SH3 domain containing adaptor proteins. In *Drosophila melanogaster*, ITSN is required to regulate synaptic morphology, to facilitate efficient synaptic vesicle recycling and for viability. Here, we report our genetic analysis of *Caenorhabditis elegans* intersectin. In contrast to *Drosophila, C. elegans itsn-1* protein null mutants are viable and display grossly normal locomotion and development. However, motor neurons in these mutants show a dramatic increase in large irregular vesicles and accumulate membrane-associated vesicles at putative endocytic hotspots, approximately 300 nm from the presynaptic density. This defect occurs precisely where endogenous ITSN-1 protein localizes in wild-type animals and is associated with a significant reduction in synaptic vesicle number and reduced frequency of endogenous synaptic events at neuromuscular junctions (NMJs). ITSN-1 forms a stable complex with EHS-1 (Eps15) and is expressed at reduced levels in *ehs-1* mutants. Thus, ITSN-1 together with EHS-1, coordinate vesicle recycling at *C. elegans* NMJs. We also found that both *itsn-1* and *ehs-1* mutants show poor viability and growth in a *Disabled (dab-1)* null mutant background. These results show for the first time that intersectin and Eps15 proteins function in the same genetic pathway, and appear to function synergistically with the clathrin-coat-associated sorting protein, Disabled, for viability.

Keywords

Dab; endocytosis; Eps15; intersectin; synaptic vesicle

*Corresponding author: Sean E. Egan, segan@sickkids.ca.

Genetic studies in organisms from yeast to mice have helped to define key elements in membrane-trafficking pathways, including an important role for EH domain proteins in several contexts (1–4). Some EH domain proteins, however, are not conserved in yeast. This may be related to the fact that specialized endocytic processes, like synaptic vesicle recycling and phagocytosis occur in multicellular organisms but not in yeast. Membrane trafficking and the specific function of these EH domain proteins are therefore, best studied in genetic model organisms such as *Caenorhabditis elegans* and *Drosophila melanogaster*. Salcini et al. have defined a role for an EH domain encoding gene, *ehs-1*, the *C. elegans* orthologue of vertebrate *Eps15*, in synaptic vesicle recycling (5). *rme-1*, the nematode orthologue of mammalian EHD family genes, which code for a specific subclass of EH domain-containing proteins, is required for recycling of endocytic cargo derived from the basolateral surface of polarized intestinal cells (6). ITSNs, which contain EH domains as well as an extended coiled-coiled domain and multiple SH3 domains are also specific to multicellular organisms (7–13). ITSNs are thought to co-ordinate endocytosis, exocytosis and signaling (11,14,15). In *D. melanogaster*, ITSN is required in the nervous system for viability of the organism, for regulation of synaptic growth and morphology as well as for synaptic vesicle recycling (16,17).

Disabled-family clathrin-coat-associated sorting proteins (CLASPs) (18) are another class of conserved regulators of endocytosis. For example, disabled proteins control the internalization of lipoprotein receptors in organisms ranging from *C. elegans* (DAB-1) (19–21) to mammals (Dab1 and Dab2) (22–25). The disabled proteins contain an N-terminal PTB domain and a number of small peptide motifs that mediate interaction with proteins and complexes implicated in endocytosis including clathrin and adaptor protein 2 (AP2). CLASPs and other endocytic proteins, such as autosomal recessive hypercholesterolemia (ARH), can play overlapping functions with respect to the internalization of cargo (18,24–26), and the importance of individual endocytic proteins depends very much on expression of these redundant proteins in a given cell type (27,28).

To define functions of ITSN, we have analyzed the phenotype of an *itsn-1* deletion mutant in *C. elegans*. We demonstrate that protein null *itsn-1* mutants are viable with grossly normal locomotion and development, but show defective synaptic vesicle recycling at the neuromuscular junction (NMJ), resulting in abnormal accumulation of large irregular vesicles, excess contacting vesicles in known endocytic hotspots within the synapse and reduced miniature postsynaptic current (mPSC) frequencies. Like their mammalian orthologues (8), *C. elegans* ITSN-1 forms a stable complex with EHS-1 *in vivo*, and ITSN-1 protein accumulation is dramatically reduced in *ehs-1* loss-of-function mutants, suggesting that these proteins function together. As *itsn-1* is not essential in *C. elegans*, we further performed genetic analyses to identify genes that may function synergistically with ITSN-1 for viability. We observed, a strong genetic interaction between *itsn-1* and *dab-1 (Disabled-1)* deletion mutants. Unlike *itsn-1, ehs-1* and *dab-1* single mutants as well as *itsn-1;ehs-1* double mutants, *itsn-1;dab-1* as well as *ehs-1;dab-1* double mutants showed extremely poor growth and viability. This synthetic lethality suggests that in *C. elegans*, the ITSN-1/EHS-1 complex may regulate membrane trafficking essential for viability in a *dab-1* sensitized background.

Results

C. elegans intersectin, ITSN-1, is highly expressed in the nervous system and localizes to the NMJ

The *C. elegans* genome codes for a single intersectin orthologue, *itsn-1*, which like the short isoforms of *Itsn1* and *Itsn2* in mammals, has two N-terminal EH domains, a central coiled coil domain, five C-terminal SH3 domains and four predicted α-adaptin interaction motifs

(Figure 1 and Figure S1) (29). To determine where ITSN-1 is expressed, we first cloned a 1.1 kb genomic DNA fragment upstream of the *itsn-1* start codon. Driving a nuclear green fluorescent protein (GFP) reporter, this presumptive *itsn-1* promoter activated expression prominently in the nervous system of larvae and adults (Figure 2A – D). The strongest expression was observed in interneurons and motor neurons as well as in some vulva cells and unidentified cells in the tail.

The National Bioresource project isolated a knockout mutant of *C. elegans itsn-1*, termed *tm725*, which has an 848 bp out-of-frame deletion starting within the second exon, and is predicted to code for a peptide including the first 149 residues of ITSN-1 followed by two out-of-frame residues (Figure 1 and Figure S1). This N-terminal peptide contains only one of the EH domains, and therefore, is predicted to be a severe loss-of-function or null allele. To determine whether *itsn-1 (tm725)* was a molecular null, we generated and purified polyclonal antibodies against a large N-terminus fragment of the protein including both EH domains. These antibodies were highly specific. They did not recognize any major bands on Western blots of lysates prepared from *tm725* deletion mutant animals (Figure 3A), and did not stain the deletion mutants in whole mount immunofluorescent experiments (data not shown). Whole mount immunofluorescent staining of wild-type animals with the ITSN-1 antibody revealed a high-level of expression throughout the nervous system (Figure 3B,C), with staining concentrated in punctate structures within neurons, most prominently in the nerve ring and in the ventral and dorsal nerve cords.

To further define where the protein is localized in these neurons, we examined ITSN-1 localization in relationship to synapses. To do so, we first generated a functional (see below) GFP-tagged ITSN-1 construct with the fluorescent tag fused to the *itsn-1* start codon in the context of an *itsn-1* genomic clone. As with the endogenous protein, GFP: :ITSN-1 was also localized in punctate structures throughout the nervous system in transgenic animals carrying a stable integrated array of this construct (data not shown). Double fluorescent labeling between GFP and various synaptic proteins revealed that GFP: :ITSN-1 showed a high degree of colocalization with synaptotagmin (Figure 3D) and other synaptic vesicle markers (data not shown), suggesting that ITSN-1 localizes to synapses, at vesicle rich regions.

ITSN-1 is localized to endocytic zones within the NMJ of wild-type animals and large irregular vesicles accumulate in *itsn-1* mutants

To define the precise subcellular localization of ITSN-1 protein at the NMJ, we performed immunoelectron microscopy on ultrathin sections prepared from wild-type animals fixed by high-pressure freezing, which preserves synapses for high-resolution immunocytochemical and morphometric analysis (30,31). Using immunogold-labeled secondary antibodies, the most densely labeled areas were distal from the presynaptic density (PD), in that membrane-associated beads accumulated 200–400 nm from the PD (Figure 4).This area coincides with the periactive zone, a region implicated in synaptic vesicle endocytosis (30).

We next compared the NMJ morphology of *itsn-1(tm725)* mutant and wild-type animals by transmission electron microscopy (Figure 5). As above, animals were subjected to rapid fix through high-pressure freezing to preserve synaptic structure under physiological conditions. In *itsn-1* mutants, the overall number of synaptic vesicles per synapse was significantly reduced (Figure 5A), while there was a dramatic increase in the number of large irregular vesicles (LIV) (Figure 5B, F). The number and distribution of plasma membrane contacting vesicles were also significantly altered in *itsn-1* mutants (Figure 5C–E). Specifically, a significant reduction in the total number of contacting vesicles per profile was observed (Figure 5C), with the largest reduction occurring within 100 nm of the PD (Figure 5D,E), which primarily represents the primed vesicle pool (30). In addition, there was an increase in

the proportion of contacting vesicles evident 200–500 nm away from the PD (Figure 5D,E). This region coincides with the localization of ITSN-1 (see above) as well as dynamin in wild-type animals (30). The loss of synaptic vesicles coupled with the appearance of large irregular vesicles and putative endocytic intermediates distal to the PD is characteristic of *C. elegans* mutants with impaired synaptic vesicle endocytosis/recycling, such as *unc-57*/endophilin, *unc-26*/synaptojanin and *syd-9* (32). Thus, the ultrastructural defects of *itsn-1* mutant synapses suggest that ITSN-1 is required in the endocytic zone for efficient recovery and recycling of synaptic vesicles. The loss of vesicles in the primed vesicle pool, also observed in *syd-9* mutants (30,32), may be a consequence of reduced vesicle availability as well as defective vesicle protein retrieval leading to inefficient priming.

Reduced frequency of endogenous synaptic events in *itsn-1* mutants

We next compared synaptic transmission at the NMJ in wild-type animals and *itsn-1* mutants via electrophysiological analyses. Spontaneous and evoked synaptic activities at NMJs were recorded on dissected wild-type and *itsn-1(tm725)* animals using the whole-cell voltage-clamp technique (*see Materials and Methods*). In 5 mM external calcium, *itsn-1(tm725)* mutants showed a 50% reduction of (mPSC) frequency [38.7 ± 3.6 Hz, $n = 18$ and 20.5 ± 3.6 Hz, $n = 18$ for wild-type and *itsn-1(tm725)*, respectively] with no significant change in mPSC amplitude (Figure 6A top two traces and Figure 6B). When extracellular calcium was decreased to 1 m_M, which reduces the overall number of neurotransmitter release events, the mPSC frequency was even more dramatically reduced in *itsn-1 (tm725)* mutants [21.7 ± 4.5 Hz, $n = 10$ and 4.4 ± 0.8 Hz, $n = 8$ for wild type and *itsn-1 (tm725)*, respectively] (Figure 6B). Under this condition, the mPSC amplitude was slightly reduced in mutant synapses [26.2 ± 2.2 pA $n = 10$ and 20.7 ± 0.9 pA $n = 8$ for wild type and *itsn-1(tm725)*, respectively] (Figure 6B). This slight effect is likely because of the reduced frequency of release events, leading to fewer overlapping mPSCs, which can inflate the average single event amplitude.

A reduction in mPSC frequency has also been observed in *unc-57*/endophilin and *unc-26*/synaptojanin mutants, although the mPSC frequency was more severely reduced in these mutants (by 85%) (33). To confirm that synaptic defects resulted specifically from the loss of ITSN-1 function, we generated transgenic *itsn-1 (tm725)* mutant lines carrying Piten-7-GFP: :ITSN-1-expressing extrachromosomal arrays. We compared endogenous events in transgenic progeny [*itsn-1 (tm725); Piten*-1-GFP: :ITSN-1] at 5 mM extracellular calcium to those in nontransgenic *itsn-1* progeny from the same lines [*itsn-1 (tm725)*], and to those of wild-type (N2) animals. Indeed, while all nontransgenic *itsn-1 (tm725)* mutants displayed a significantly reduced mPSC frequency (Figure 6A,C), 55% of the examined transgenic *itsn-1(tm725)* mutants carrying *Pitsn-1*-GFP: :ITSN-1 were completely rescued, showing spontaneous synaptic activity at a frequency and amplitude indistinguishable from that observed in wild-type animals (Figure 6A,C). As expected from *C. elegans* transgenic rescuing experiments, not all transgenic animals showed full rescue because of mosaic expression of the introduced transgene (34).

In contrast to the endogenous release frequency, electrical stimulation of the ventral nerve cord evoked identical responses in wild-type and *itsn-1(tm725)* animals at both calcium concentrations (Figure 6D,E). These evoked postsynaptic currents had an average amplitude of 1189 ± 125 pA ($n = 10$) and 544 ± 76 pA ($n = 10$) for wild-type and 1204 ± 137 pA ($n = 11$) and 514 ± 93 pA ($n = 5$) for *itsn-1 (tm725)* animals at 5 and 1 mM Ca^{++}, respectively. The kinetics of the evoked response in wild-type and *itsn-1* mutants was also similar. Fitting the decrease of evoked responses at 5 mM Ca^{++} with a single exponential function revealed averaged time constant values of 6.5 ± 0.6 ms for wild-type against 5.6 ± 0.7 for *tm725* mutants. Time-to-peak was 2.4 ± 0.2 ms for wild-type and 2.5 ± 0.2 ms for *itsn-1 (tm725)* mutants. Therefore, in contrast to *unc-57* and *unc-26* mutants, where defective synaptic

vesicle recycling also causes a significant decrease in evoked response, *itsn-1* mutants are able to maintain normal evoked release (33). Similarly, repeat stimulation results in a faster depression of evoked trains in *unc-57* and *unc-26* (33) mutants, but not itsn-1 mutants (data not shown). These data reflect the milder endocytic phenotype of *itsn-1* mutants, both in terms of reduced vesicle number as well as less severe reduction in mini frequency.

EHS-1 and ITSN-1 form a stable protein complex *in vivo*

To purify ITSN-1 complexes from *C. elegans* lysates, we generated an anti-ITSN-1 column using our affinity-purified rabbit antisera. A number of protein bands were eluted from this column and the corresponding proteins identified using mass spectrometry. Two of these represented ITSN-1 and EHS-1, respectively (Figure S2 and Table S1). Potential ITSN-1 partners were also identified in yeast two-hybrid screens using the EH domain containing N-terminus, the coiled-coil domain and the SH3 domain containing C-terminus as baits, and a *C. elegans* mixed stage library as prey (Table S2). Again, EHS-1 was identified through its affinity for the central coiled-coil domain of ITSN-1. These results suggest that EHS-1 and ITSN-1 form a stable protein complex in *C. elegans*, consistent with our previous discovery of the intersectin-Eps15 complexes in mammalian cells (8). This complex of two EH domain-containing proteins is likely analogous to the protein scaffold that is an important regulator of endocytosis in yeast (35,36).

To test for a functional relationship between ITSN-1 and EHS-1 *in vivo*, we analyzed ITSN-1 expression in the *ehs-1* null mutants, *ok146*. ITSN-1 protein expression was dramatically reduced in *ehs-1* mutant animals (Figure 7A,B), while *itsn-1* mRNA levels were unaffected (Figure 7C). This suggests that *itsn-1* translation, or more likely, protein stability is reduced in the absence of its EHS-1 partner. This phenomenon is reminiscent of the reduced accumulation of partner proteins that occurs in NMJs of the *Drosophila* intersectin mutants (16,17). We next tested whether reduced ITSN-1 protein level was specific to the *ehs-1* mutants by testing for alterations in ITSN-1 protein expression in other endocytic mutants. Interestingly, the ITSN-1 level appeared normal in *unc-11, unc-26, unc57and dab-1* mutants (Figure 7D).

Itsn-1 and *ehs-1* show a strong genetic interaction with *disabled/dab-1*

All aspects of synaptic defects of *itsn-1* protein null mutants are significantly weaker than that observed in mutants of *unc-57*/endophilin and *unc-26*/synaptojanin. While severe loss-of-function alleles for *unc-57* and *unc-26* show strong locomotion defects and slow growth (33), *itsn-1* protein null mutants display no gross locomotion defects and normal development. This is also in contrast to the situation in *Drosophila*, where *itsn* is an essential gene. Given that *itsn-1* encodes the sole *C. elegans* ITSN family protein, additional proteins must function in parallel to regulate endocytosis in this organism. To identify such components, we performed double mutant analysis with a number of candidate genes that are known or predicted to be required for endocytosis or other postulated ITSN-dependent processes (Table 1). We looked for mutations that modified the phenotypes of *itsn-1* mutants. These analyses were performed using either the *itsn-1*(*tm725*) mutant and/or a second *itsn-1* deletion allele, *ok268* (Figure S1). Identical results were obtained in all cases where both *itsn-1* mutants were analyzed (see below), suggesting that there is no allelic influence for the exhibited phenotypes.

Most double mutants display additive phenotypes, suggesting a lack of obvious genetic interactions. An exception was observed with *itsn-1;dab-1* double mutants. The *dab-1* gene codes for the *C. elegans* homologue of a CLASP-family protein disabled. The *gk291* a deletion allele for *dab-1* behaves as a genetic null and removes its conserved PTB domain, causing a severe, if not complete loss of function of the DAB-1 protein (21). The *dab-1*

single mutants show mild growth and egg-laying defects, and uncoordinated locomotion. However, these mutants were fertile and had near normal brood sizes. In contrast, *itsn-1;dab-1* double mutants showed L1-L4 larval arrest with severe and progressive paralysis. The small number of escapers and their small brood size in fact prevented maintenance of the double mutant stocks. Interestingly, DAB-1 was identified in our yeast two-hybrid screen through its affinity for the N-terminal EH domain-containing region of ITSN-1 (Table S2). NPF motifs are known EH domain ligands (37), and therefore, the interaction detected in yeast was likely mediated by the NPF motifs in DAB-1.

As ITSN-1 forms a stable complex with EHS-1, and ITSN-1 protein accumulation is dependent on the presence of *ehs-1* (Figure 7), we next tested whether *ehs-1* also showed the same genetic interaction with *dab-1*. The *ehs-1;dab-1* double mutant animals were also very sick and indistinguishable from *itsn-1;dab-1* double mutants (Table 1). This is in contrast to our observation that *ehs-1;itsn-1* double deletion mutants behave essentially identical to *ehs-1* or *itsn-1* single mutants for locomotion and growth (data not shown). The synthetic lethality observed in *itsn-1; dab-1* and *ehs-1;dab-1* double mutants is thus consistent with the ITSN-1/EHS-1 protein complex functioning in the same genetic pathway, while DAB-1 participates in a biological pathway that functions synergistically or cooperatively for viability.

Discussion

Synaptic vesicle recycling is a specialized form of clathrin-mediated endocytosis, believed to involve the coordinated assembly and temporal reorganization of macromolecular complexes linked to AP2 and clathrin, to the lipid phos-phatidylinositol 4,5-bisphosphate (PIP2) and to specific membrane cargo (38). AP2, clathrin and their cargo concentrate at the membrane, where they form a lattice network that recruits additional proteins leading to membrane curvature responsible for vesicle budding. Finally, additional proteins are recruited to facilitate vesicle scission and uncoating. As noted above, the membrane-binding proteins AP180 (UNC-11) and endophilin (UNC-57) as well as the PIP2-phosphatase synaptojanin (UNC-26), all play a major role in synaptic vesicle recycling, and as a result, mutations in these *C. elegans* genes cause an uncoordinated phenotype and slow growth.

In *Drosophila*, ITSN is also required to facilitate efficient synaptic vesicle recycling (16,17). Based primarily on tissue culture studies, a number of functions have been proposed for mammalian Itsn-1 and ltsn-2, including regulation of the actin cytoskeleton, exocytosis, caveolae internalization and activation of cytoplasmic signaling pathways (7,13,15,39–43). Here, we report that the sole *C. elegans* ITSN shares a similar function to that observed in *Drosophila* in coordinating efficient vesicle recycling. Previous studies in *C. elegans* have shown that *unc-57/ endophilin* and *unc-26/synaptojanin* mutants have a dramatically reduced number of synaptic vesicles at the active zone and a dramatically increased number of endocytic pits, clathrin-coated vesicles, ‘string-of-pearls’ vesicle structures and large irregular-shaped vesicles (LIV) or cisternae. These two mutants also show dramatically reduced mPSC frequency as well as reduced evoked postsynaptic current amplitude, uncoordinated movement and delayed development (33). The *unc-11/AP-180* mutant also accumulates large empty synaptic vesicles (44,45). The *itsn-1* mutant studied here displayed several of these characteristic defects of endocytic mutants, including; a reduced number of synaptic vesicles, a significant accumulation of large irregular vesicles and reduced mPSC frequency. These data indicate that ITSN-1 facilitates efficient vesicle recycling and endogenous synaptic activity at NMJs. However, unlike *unc-11, unc-26* and *unc-57, itsn-1* mutants display well-coordinated locomotion on plates suggesting that ITSN-1 plays a less prominent role in synaptic vesicle endocytosis than these other genes.

Locomotion on plates is normal for *itsn-1;ehs-1* double mutants, as it is for *itsn-1* and *ehs-1* single mutants (5). Given that *itsn-1* and *ehs-1* alleles are both deletions predicted to severely disrupt protein expression and function, their genetic interactions are most consistent with a model whereby ITSN-1 and EHS-1 function in the same pathway. Furthermore, our data indicate that their contribution to vesicle recycling is regulatory rather than essential under standard conditions. Because the *itsn-1* deletion mutation does not obviously enhance the behavioral defects of *unc-26, unc-57* or *unc-11* loss-of-function mutants (data not shown), the ITSN-1/EHS-1 protein complex is likely to function in the same basic pathway as these core endocytic components. This is supported by an observed reduction of GFP: :UNC26/synaptojanin protein accumulation in *itsn-1* mutants suggesting that recruitment of synaptojanin to the nascent clathrin-coated synaptic vesicle is partially dependent on ITSN-1 (Figure S3). However, sufficient recruitment and/or stabilization of synaptojanin as well as endophilin and dynamin must still occur in the absence of ITSN-1 or EHS-1 in *C. elegans* because motility is not adversely affected in either mutant. This is in contrast to the situation in *Drosophila*, where synaptojanin, endophilin and dynamin, are strongly destabilized and the recycling system essentially fails.

We, therefore, propose that ITSN-1/EHS-1 complexes serve as a nonessential scaffold to facilitate interactions among endocytic components, and to promote efficient synaptic vesicle recovery at the *C. elegans* NMJ. Supportive of this model, our proteomic analyses and yeast two-hybrid screen identified a number of candidate ITSN-1-binding proteins (Tables S1 and S2), among which several are known to bind ITSN or EPS15 in other species, or are known to play a critical role in the endocytic pathway (Figure S4). For example, AP180, epsin and connecdenn are implicated in cargo recognition, clathrin recruitment and vesicle budding; dynamin is required for vesicle scission and synaptojanin is implicated in various endocytic stages including vesicle uncoating (38).

The CLASP proteins DAB-1 and NUM-1/Numb (37,46), implicated in the recruitment of AP2 to specific cargo, are also candidate ITSN-1/EHS-1-binding partners. Interestingly, *dab-1* was identified in our synthetic sick/lethal screen. Recent analysis of the *C. elegans dab-1* mutant has shown that this gene plays a number of important roles in development (19–21). In addition, this gene is required for viability in *C. elegans* in combination with components of the AP3 clathrin adaptor protein complex (21).In mammals, disabled proteins regulate lipoprotein receptor trafficking, and this has an impact on a number of vital signaling pathways (22,24,49–55). While DAB-1 has affinity for ITSN-1 (Table S2), it was not identified as a stable ITSN-1 partner by our immunopurification screen (Table S1), suggesting CLASP proteins may associate only transiently with ITSN/EPS15 complexes during endocytic retrieval of cargo. The synthetic genetic interaction between *itsn-1* and *dab-1* (as well as between *ehs-1* and *dab-1)* reveals that ITSN-1 and EHS-1 become essential in a *dab-1* null background. This synthetic lethality, therefore, may reflect the sensitization of *dab-1* mutants to defects in other membrane trafficking pathways during development. One potential mechanism for the genetic interaction observed here could be that DAB-1 and EHS-1/ITSN-1 pathways share specific cargo for internalization, and that such cargoes are required for viability. It will be important in future studies to analyze the *itsn-1;dab-1* double mutant phenotype to define the shared function of these genes, and how they coordinate membrane trafficking during development.

In summary, we have shown that *itsn-1* and *ehs-1* function in the same pathway and that there encoded proteins interact *in vivo*. We have further shown that the ITSN-1/ EHS-1 complex plays a nonessential, regulatory role in synaptic vesicle endocytosis likely through its interaction with the core endocytic machinery. Finally, the genetic interactions between *itsn-1, ehs-1* and *dab-1* are consistent with the ITSN-1/EHS-1 complex functioning either synergistically or cooperatively with DAB-1 for survival.

During preparation of this manuscript for submission, Rose et al. published a study on *C. elegans itsn-1*. In this report, *itsn-1* mutants were found to be hypersensitive to the acetylcholine esterase inhibitor, aldicarb. These authors also noted that *itsn-1* and *ehs-1* mutants show opposite aldicarb sensitivity phenotypes, and opposite genetic interactions with dynamin mutants. These data were interpreted to suggest that ITSN-1 inhibits synaptic transmission. Our data, based on electrophysiological examination of synaptic transmission as well as ultrastructural analysis of *itsn-1* mutants, strongly suggest that ITSN-1 and EHS-1 both promote endocytosis of synaptic vesicles. *itsn-1* and *ehs-1* mutants also show the same synthetic sick/lethal genetic interaction with *dab-1*. We, therefore, favor the interpretation that *C. elegans* ITSN-1 and EHS-1 are partners that function together to enhance synaptic vesicle recovery from the periactive zone, a role consistent with that of their fly homologues (47).

Materials and Methods

C. elegans handlings and strains

Methods for the handling and culturing of *C. elegans* are as described previously (48). The Bristol strain N2 was used as wild-type control in each experiment. A number of strains studied in this manuscript, including the ok268 *itsn-1 (ok268)* mutant, were generated by the *C. elegans Gene Knockout Consortium* and provided by the *Caenorhabditis* Genetics Center (University of Minnesota, St Paul, Minnesota, USA). The *itsn-1(tm725)* and *reps-1(tm2156)* deletion mutants were generated and provided by Shohei Mitani of the Japanese National Bioresource project (Tokyo Women's Medical University School of Medicine, Tokyo, Japan). The *itsn-1, ehs-1* and *dab-1* mutant strains were backcrossed against N2 animals six times for this study.

Plasmids construction and transgenic strain

The *itsn-1* genomic DNA [7867 nucleotide (nt) sequence from nt 218489 to nt 226356 in Y116A8C], including 1.1 kb of promoter sequences upstream of the gene and the complete coding sequence, were polymerase chain reaction (PCR)-amplified as five pieces. All exons were sequenced to rule out the possibility of PCR-generated errors. For our promoter fusion construct, nt 218489–219590 in YAC Y116A8C were cloned into *Xba*I/*Sma*I-digested pPD95.67 nuclear EGFP expressing reporter plasmid (from A. Fire). For our translational GFP fusion construct, the coding sequence for GFP from pEGFP-C1 (Clontech) was inserted immediately upstream of the first *itsn-1* codon in the context of *itsn-1* genomic DNA in a pBKS vector (Stratagene). The promoter fusion and translational fusion plasmids were co-injected with pRF4 as a transformation marker into N2. Integrated animals were obtained by ultraviolet radiation and were backcrossed to wild-type N2 animals six times.

Antibody generation, Western blot analysis and whole-mount antibody staining

To generate antibodies against *C. elegans* ITSN-1, sequences coding for its N-terminal 333 amino acids were PCR amplified using an ESTest clone *yk1011g8* as template (a gift from Yuji Kohara, National Institute of Genetics, Mishima, Japan), and cloned into *Bam*HI/*Xho*I-digested pGEX-4T-3 (Amersham Biosciences). The resulting plasmid was transformed into bacteria and glutathione S-transferase (GST) ITSN-1 fusion protein purified on Glutathione Sepharose 4B beads (Amersham Biosciences). The fusion protein was then used to immunize rabbits. Resulting antisera were cleared on a GST column followed by affinity purification on a GST ITSN-1 fusion protein column (Pharmacia). Rabbit anti-UNC-10, rabbit anti-SNT-1, rabbit anti-SNB-1 (Mike Nonet, Washington University at St Louis) and mouse monoclonal anti-β-tubulin antibodies (Developmental Studies Hybridoma Bank, University of Iowa) have been previously described. Mouse anti-enhanced green fluorescent protein (EGFP) (3E6), Alexa Fluor 488 donkey anti-mouse immunoglobulin G (IgG) and

Alexa Fluor 594 chicken anti-rabbit IgG were purchased from Molecular Probes. Western blot analysis was performed on mixed stage worms. Briefly, packed worms were rapidly frozen in liquid N2 and then crushed with mortar and pestle, followed by incubation in lysis buffer. Resulting lysates were run on 7.5% polyacrylamide gel electrophoresis gels and transferred to nitrocellulose membranes. Enhanced chemiluminescence detection system was used according to manufacturer's instruction (Amersham). Whole-mount antibody staining was performed as described (49).

Light and electron microscopy

Live transgenic worms were placed onto a dry agarose pad in the present of M9 buffer for imaging. Whole-mount-stained worms were mounted with fluorescent mounting medium (DAKO S3023). Confocal microscope (ZEISS LSM 510 META) with 63× oil immersed objective was used to visualize samples. For Nomarski images, we used a Leica DMRA2 microscope with a 63× oil immersed objective. Electron microscopy was performed as previously described (30). Eighteen synapses were analyzed for immunoelectron microscopy as shown in Figure 4, the ITSN-1 antibody was used at a dilution of 1 : 30, and secondary 15-nm gold bead-conjugated antibody at 1 : 100. For morphometry, as shown in Figure 5, 8 wild-type synapses and 10 *itsn-1 (tm725) itsn-1* mutant synapses were analyzed. Large irregular vesicles were identified and quantified on the basis of contrast (these structures were typically empty, in comparison to synaptic vesicles and large dense core vesicles), size (LIV were bigger than synaptic vesicles, which range from 26 to 30 nM diameter and large dense core vesicle) and shape (some LIV had an irregular shape, especially the very large ones).

Electrophysiology

Methods were essentially as described (50,51). Animals were glued (52,53) with Histoacryl Glue (B. Braun) along their dorsal side on Sylgard-coated coverslips (Dow Corning) and cut open along the glue under extracellular recording solution (54). Once the internal organs were dilacerated and removed, the cuticle flap was glued back and the prep was exposed to 0.4 mg/mL collagenase for about 10 seconds. The apparent integrity of the anterior ventral medial body muscle and the ventral nerve cord could then be assessed under a microscope equipped with Nomarski DIC. Muscle cells were patched using fire-polished, 4 mΩ resistant borosilicate pipettes (World Precision Instruments), clamped at −60 mV throughout the experiments using an Axopatch 1D amplifier (Molecular Devices) and recorded using the whole-cell patch-clamp technique within 5 min following dissection. The recording solutions were as described. Signals were filtered at 5 kHz, digitized via a Digidata 1322A acquisition card (Molecular Devices), and data acquired and analyzed using PCLAMP software (Molecular Devices) and graphed with Excel (Microsoft). After 10–60 seconds (54) of spontaneous event recordings, a highly resistant fire-polished electrode filled with 3 mM KCI was brought close to the ventral nerve cord, anterior to the recorded muscle cell, and a 1 millisecond depolarizing current was applied.

ITSN-1 complex isolation and MALDI-TOF mass spectrometry

Lysate prepared from 1 mL of packed mix-stage worms was loaded onto an affinity-purified rabbit anti-ITSN-1 mini-column. After multiple washes with PBS, ITSN complexes were eluted from the column and concentrated with centricon-10 concentrators (Amicon). These complexes were then separated on 4–15% Tris–HCI gradient gels (Bio-Rad Laboratories), protein bands virtualized by Coomassie blue staining, and bands of interest excised. In-gel digestion with trypsin, extraction and purification of tryptic fragments were followed as described previously (55). The purified tryptic peptides were analyzed by MALDI-TOF ((Matrix-assisted laser desorption/ionization)-(time-of-flight)) mass spectrometry and/or Tandem (MS-MS) mass spectrometry.

Generation of *itsn-1* bait plasmids and yeast two-hybrid screen

For pPC97-ITSN-1-EH: an ITSN-1 EH domain fragment (encoding amino acid 1–275) was PCR amplified using *itsn-1* cDNA clone yk1011g8 as template, sequenced and cloned into *Sal*I-*Not*I-digested pPC97 vector in frame with the GAL4 DNA-binding domain. For pPC97-ITSN-1-C-C: reverse transcriptase PCR (RT-PCR) was performed to obtain an ITSN-1 coiled-coil domain fragment (encoding amino acid 269–663) using wild-type (N2) total RNA. The fragment was sequenced and cloned into *Xho*I-*Not*I-digested pPC97 vector in frame with the GAL4 DNA-binding domain. For pPC97-ITSN-1-SH3: RT-PCR was performed to obtain the ITSN-1 C-terminal SH3-domain containing fragment (encoding amino acid 657–1085) using wild-type (N2) total RNA. The resulting cDNA was sequenced and cloned into *Sal*I-*Not*I-digested pPC97 vector in frame with the GAL4 DNA-binding domain. Two-hybrid screen of the yeast open reading frame (ORF) activation domain library were performed as per report previously (56) using 3 mM 3-amino-1,2,4-triazol for selection. The library that we screened was generated from mixed stage worm culture cDNA.

Examination of *itsn-1* mRNA level in wild-type N2 and *ok 146* animals

Total RNA of mix-stage animals was obtained from N2 and *ok146* using Trizol reagent (Invitrogen). The *itsn-1* mRNA level was determined by semiquantitative RT-PCR. A 0.25 μg of total RNA was used to perform one-step RT-PCR (Invitrogen) as described in manufactory's instruction. PCR primers for *itsn-1* were: sense-5′-GAGTCGACCGCGTTCAATATTCATGA-CACT-3′, antisense-5′-GAGCGGCCGCTTATTGCTGCTGAACATAAT-3′, which flanked the SH3 domain coding region of *itsn-1* mRNA. All PCR reactions were standardized using *C. elegans* eukaryotic initiation factor 4A homologue (CelF) as a control (sense primer-5′-GATGTGAACGTATCTTCGGTG-3′ and antisense primer-5′-GTTGATAACAAGTGAGACCTGTTG-3′) as described previously (57).

Supplementary Material

Refer to Web version on PubMed Central for supplementary material.

Acknowledgments

S. E. E.'s laboratory has been supported by funds from the Canadian Institutes for Health Research (CIHR). K. X. has been supported by a CIHR fellowship. M. B. and E. H. L. were supported by CIHR grants awarded to M. Z., and E. O. G. was supported by NIH grants awarded to J. E.R. The authors would like to thank M. Nonet, A. Alfonso and J. Cooper for antibodies, and members of the Egan and Zhen laboratories for valuable advice and encouragement. Also, we thank Lisa Salcini and Pier Paolo Di Fiore for communicating results of their studies on *itsn-1* prior to publication, as well as the *C. elegans* Gene knockout Consortium, the *Caenorhabditis* Genetics Center, the Japanese National Bioresource project, J. Withee and G. Garriga for providing strains.

References

1. Hurley JH, Emr SD. The ESCRT complexes: structure and mechanism of a membrane-trafficking network. Annu Rev Biophys Biomol Struct. 2006; 35:277–298. [PubMed: 16689637]
2. Miliaras NB, Park JH, Wendland B. The function of the endocytic scaffold protein Pan1p depends on multiple domains. Traffic. 2004; 5:963–978. [PubMed: 15522098]
3. Miliaras NB, Wendland B. EH proteins: multivalent regulators of endocytosis (and other pathways). Cell Biochem Biophys. 2004; 41:295–318. [PubMed: 15475615]
4. Polo S, Confalonieri S, Salcini AE, Di Fiore PP. EH and UIM: endocytosis and more. Sci STKE. 2003; 2003:re17. [PubMed: 14679291]

5. Salcini AE, Hilliard MA, Croce A, Arbucci S, Luzzi P, Tacchetti C, Daniell L, De Camilli P, Pelicci PG, Di Fiore PP, Bazzicalupo P. The Eps 15 C. elegans homologue EHS-1 is implicated in synaptic vesicle recycling. Nat Cell Biol. 2001; 3:755–760. [PubMed: 11483962]
6. Grant B, Zhang Y, Paupard M-C, Lin SX, Hall DH, Hirsh D. Evidence that RME-1. a conserved C. elegans EH-domain protein, functions in endocytic recycling. Nat Cell Biol. 2001; 3:573–579. [PubMed: 11389442]
7. Sengar AS, Egan SE. Itsn2. UCSD-Nature Molecule Pages. 2006
8. Sengar AS, Wang W, Bishay J, Cohen S, Egan SE. The EH and SH3 domain Ese proteins regulate endocytosis by linking to dynamin and Eps15. EMBO J. 1999; 18:1159–1171. [PubMed: 10064583]
9. Roos J, Kelly RB. Dap160, a neural-specific Eps15 homology and multiple SH3 domain-containing protein that interacts with Drosophila dynamin. J Biol Chem. 1998; 273:19108–19119. [PubMed: 9668096]
10. Guipponi M, Scott HS, Chen H, Schebesta A, Rossier C, Antonarakis SE. Two isoforms of a human intersectin (ITSN) protein are produced by brain-specific alternative splicing in of a stop codon. Genomics. 1998; 53:369–376. [PubMed: 9799604]
11. Okamoto M, Schoch S, Sudhof TC. EHSHI/intersectin, a protein that contains EH and SH3 domains and binds to dynamin and SNAP-25. J Biol Chem. 1999; 274:18446–18454. [PubMed: 10373452]
12. Yamabhai M, Hoffman NG, Hardison NL, McPherson PS, Castagnoli L, Cesareni G, Kay BK. Intersectin, a novel adaptor protein with two epsl 5 homology and five src homology 3 domains. J Biol Chem. 1998; 273:31401–31407. [PubMed: 9813051]
13. Sengar AS, Egan SE. Itsnl. UCSD-Nature Molecule Pages. 2005
14. Broadie K. Synapse scaffolding: intersection of endocytosis and growth. Curr Biol. 2004; 14:R853–R855. [PubMed: 15458667]
15. O'Bryan JP, Mohney RP, Oldham CE. Mitogenesis and endocytosis: what's at the intersection? Oncogene. 2001; 20:6300–6308. [PubMed: 11607832]
16. Koh TW, Verstreken P, Bellen HJ. Dap160/intersectin acts as a stabilizing scaffold required for synaptic development and vesicle endocytosis. Neuron. 2004; 43:193–205. [PubMed: 15260956]
17. Marie B, Sweeney ST, Poskanzer KE, Roos J, Kelly RB, Davis GW. Dap160/intersectin scaffolds the periactive zone to achieve high-fidelity endocytosis and normal synaptic growth. Neuron. 2004; 43:207–219. [PubMed: 15260957]
18. Traub LM, Lukacs GL. Decoding ubiquitin sorting signals for clathrin-dependent endocytosis by CLASPs. J Cell Sci. 2007; 120:543–553. [PubMed: 17287393]
19. Kamikura DM, Cooper JA. Lipoprotein receptors and a disabled family cytoplasmic adaptor protein regulate EGL-17/FGF export in C. elegans. Genes Dev. 2003; 17:2798–2811. [PubMed: 14630941]
20. Kamikura DM, Cooper JA. Clathrin interaction and subcellular localization of Ce-DAB-1, an adaptor for protein secretion in Caenorhabditis elegans. Traffic. 2006; 7:324–336. [PubMed: 16497226]
21. Holmes A, Flett A, Coudreuse D, Korswagen HC, Pettitt JC. elegans Disabled is required for cell-type specific endocytosis and is essential in animals lacking the AP-3 adaptor complex. J Cell Sci. 2007; 120:2741–2751. [PubMed: 17636000]
22. Maurer ME, Cooper JA. Endocytosis of megalin by visceral endoderm cells requires the Dab2 adaptor protein. J Cell Sci. 2005; 118:5345–5355. [PubMed: 16263760]
23. Morimura T, Hattori M, Ogawa M, Mikoshiba K. Disabledl regulates the intracellular trafficking of reelin receptors. J Biol Chem. 2005; 280:16901–16908. [PubMed: 15718228]
24. Stolt PC, Bock HH. Modulation of lipoprotein receptor functions by intracellular adaptor proteins. Cell Signal. 2006; 18:1560–1571. [PubMed: 16725309]
25. Keyel PA, Mishra SK, Roth R, Heuser JE, Watkins SC, Traub LM. A single common portal for clathrin-mediated endocytosis of distinct cargo governed by cargo-selective adaptors. Mol Biol Cell. 2006; 17:4300–4317. [PubMed: 16870701]
26. Garcia CK, Wilund K, Arca M, Zuliani G, Fellin R, Maioli M, Calandra S, Bertolini S, Cossu F, Grishin N, Barnes R, Cohen JC, Hobbs HH. Autosomal recessive hypercholesterolemia caused by

mutations in a putative LDL receptor adaptor protein. Science. 2001; 292:1394–1398. [PubMed: 11326085]

27. Shih SC, Katzmann DJ, Schnell JD, Sutanto M, Emr SD, Hicke L. Epsins and Vps27p/Hrs contain ubiquitin-binding domains that function in receptor endocytosis. Nat Cell Biol. 2002; 4:389–393. [PubMed: 11988742]
28. Sigismund S, Woelk T, Puri C, Maspero E, Tacchetti C, Transidico P, Di Fiore PP, Polo S. Clathrin-independent endocytosis of ubiquitinated cargos. Proc Natl Acad Sci U S A. 2005; 102:2760–2765. [PubMed: 15701692]
29. Praefcke GJ, Ford MG, Schmid EM, Olesen LE, Gallop JL, Peak-Chew SY, Vallis Y, Babu MM, Mills IG, McMahon HT. Evolving nature of the AP2 alpha-appendage hub during clathrin-coated vesicle endocytosis. EMBO J. 2004; 23:4371–4383. [PubMed: 15496985]
30. Weimer RM, Gracheva EO, Meyrignac O, Miller KG, Richmond JE, Bessereau JL. UNC-13 and UNC-10/rim localize synaptic vesicles to specific membrane domains. J Neurosci. 2006; 26:8040–8047. [PubMed: 16885217]
31. Rostaing P, Weimer RM, Jorgensen EM, Triller A, Bessereau JL. Preservation of immunoreactivity and fine structure of adult C. elegans tissues using high-pressure freezing. J Histochem Cytochem. 2004; 52:1–12. [PubMed: 14688212]
32. Wang Y, Gracheva EO, Richmond J, Kawano T, Couto JM, Calarco JA, Vijayaratnam V, Jin Y, Zhen M. The C2H2 zinc-finger protein SYD-9 is a putative posttranscriptional regulator for synaptic transmission. Proc Natl Acad Sci U S A. 2006; 103:10450–10455. [PubMed: 16803962]
33. Schuske KR, Richmond JE, Matthies DS, Davis WS, Runz S, Rube DA, van der Bliek AM, Jorgensen EM. Endophilin is required for synaptic vesicle endocytosis by localizing synaptojanin. Neuron. 2003; 40:749–762. [PubMed: 14622579]
34. Stinchcomb DT, Shaw JE, Carr SH, Hirsh D. Extrachromosomal DNA transformation of Caenorhabditis elegans. Mol Cell Biol. 1985; 5:3484–3496. [PubMed: 3837845]
35. Tang HY, Xu J, Cai M. Pan 1p, End3p, and S1a1p, three yeast proteins required for normal cortical actin cytoskeleton organization, associate with each other and play essential roles in cell wall morphogenesis. Mol Cell Biol. 2000; 20:12–25. [PubMed: 10594004]
36. Wendland B, Emr SD. Pan 1p, Yeast eps15, functions as a multivalent adaptor that coordinates protein-protein interactions essential for endocytosis. J Cell Biol. 1998; 141:71–84. [PubMed: 9531549]
37. Salcini AE, Confalonieri S, Doria M, Santolini E, Tassi E, Minencova O, Cesareni G, Pelicci PG, Di Fiore PP. Binding specificity and in vivo targets of the EH domain, a novel protein-protein interaction module. Genes Dev. 1997; 11:2239–2249. [PubMed: 9303539]
38. Schmid EM, McMahon HT. Integrating molecular and network biology to decode endocytosis. Nature. 2007; 448:883–888. [PubMed: 17713526]
39. Malacombe M, Ceridono M, Calco V, Chasserot-Golaz S, McPherson PS, Bader MF, Gasman S. Intersectin-1L nucleotide exchange factor regulates secretory granule exocytosis by activating Cdc42. EMBO J. 2006; 25:3494–3503. [PubMed: 16874303]
40. Irie F, Yamaguchi Y. EphB receptors regulate dendritic spine development via intersectin, Cdc42 and N-WASP. Nat Neurosci. 2002; 5:1117–1118. [PubMed: 12389031]
41. Nishimura T, Yamaguchi T, Tokunaga A, Hara A, Hamaguchi T, Kato K, Iwamatsu A, Okano H, Kaibuchi K. Role of numb in dendritic spine development with a Cdc42 GEF intersectin and EphB2. Mol Biol Cell. 2006; 17:1273–1285. [PubMed: 16394100]
42. Predescu SA, Predescu DN, Knezevic I, Klein IK, Malik AB. Intersectin-1s regulates the mitochondrial apoptotic pathway in endothelial cells. J Biol Chem. 2007; 282:17166–17178. [PubMed: 17405881]
43. Das M, Scappini E, Martin NP, Wong KA, Dunn S, Chen YJ, Miller SL, Domin J, O'Bryan JP. Regulation of neuron survival through an intersectin (ITSN)-phosphoinositide 3'-kinase-C2{beta}-AKT pathway. Mol Cell Biol. 2007; 27:7906–7917. [PubMed: 17875942]
44. Nonet ML, Holgado AM, Brewer F, Serpe CJ, Norbeck BA, Holleran J, Wei L, Hartwieg E, Jorgensen EM, Alfonso A. UNC-11, a Caenorhabditis elegans AP180 homologue, regulates the size and protein composition of synaptic vesicles. Mol Biol Cell. 1999; 10:2343–2360. [PubMed: 10397769]

45. Harris TW, Hartwieg E, Horvitz HR, Jorgensen EM. Mutations in synaptojanin disrupt synaptic vesicle recycling. J Cell Biol. 2000; 150:589–600. [PubMed: 10931870]
46. Santolini E, Puri C, Salcini AE, Gagliani MC, Pelicci PG, Tacchetti C, Di Fiore PP. Numb is an endocytic protein. J Cell Biol. 2000; 151:1345–1352. [PubMed: 11121447]
47. Koh TW, Korolchuk VI, Wairkar YP, Jiao W, Evergren E, Pan H, Zhou Y, Venken KJ, Shupliakov O, Robinson IM, O'Kane CJ, Bellen HJ. Eps15 and Dap160 control synaptic vesicle membrane retrieval and synapse development. J Cell Biol. 2007; 178:309–322. [PubMed: 17620409]
48. Brenner S. The genetics of Caenorhabditis elegans. Genetics. 1974; 77:71–94. [PubMed: 4366476]
49. Zhen M, Jin Y. The liprin protein SYD-2 regulates the differentiation of presynaptic termini in C. elegans. Nature. 1999; 401:371–375. [PubMed: 10517634]
50. Richmond JE, Davis WS, Jorgensen EM. UNC-13 is required for synaptic vesicle fusion in C. elegans. Nat Neurosci. 1999; 2:959–964. [PubMed: 10526333]
51. Richmond JE, Jorgensen EM. One GABA two acetylcholine receptors function at the C. elegans neuromuscular junction. Nat Neurosci. 1999; 2:791–797. [PubMed: 10461217]
52. Jospin M, Jacquemond V, Mariol MC, Segalat L, Allard B. The L-type voltage-dependent Ca2+ channel EGL-19 controls body wall muscle function in Caenorhabditis elegans. J Cell Biol. 2002; 159:337–348. [PubMed: 12391025]
53. Jospin M, Mariol MC, Segalat L, Allard B. Characterization of K(+) currents using an in situ patch clamp technique in body wall muscle cells from Caenorhabditis elegans. J Physiol. 2002; 544:373–384. [PubMed: 12381812]
54. Touroutine D, Fox RM, Von Stetina SE, Burdina A, Miller DM III, Richmond JE. acr-16 encodes an essential subunit of the levamisole-resistant nicotinic receptor at the Caenorhabditis elegans neuromuscular junction. J Biol Chem. 2005; 280:27013–27021. [PubMed: 15917232]
55. Shevchenko A, Jensen ON, Podtelejnikov AV, Sagliocco F, Wilm M, Vorm O, Mortensen P, Shevchenko A, Boucherie H, Mann M. Linking genome and proteome by mass spectrometry: large-scale identification of yeast proteins from two dimensional gels. Proc Natl Acad Sci USA. 1996; 93:14440–14445. [PubMed: 8962070]
56. Uetz P, Giot L, Cagney G, Mansfield TA, Judson RS, Knight JR, Lockshon D, Narayan V, Srinivasan M, Pochart P, Qureshi-Emili A, Li Y, Godwin B, Conover D, Kalbfleisch T, et al. A comprehensive analysis of protein-protein interactions in Saccharomyces cerevisiae. Nature. 2000; 403:623–627. [PubMed: 10688190]
57. Kinoshita T, Imamura J, Nagai H, Shimotohno K. Quantification of gene expression over a wide range by the polymerase chain reaction. Anal Biochem. 1992; 206:231–235. [PubMed: 1280006]

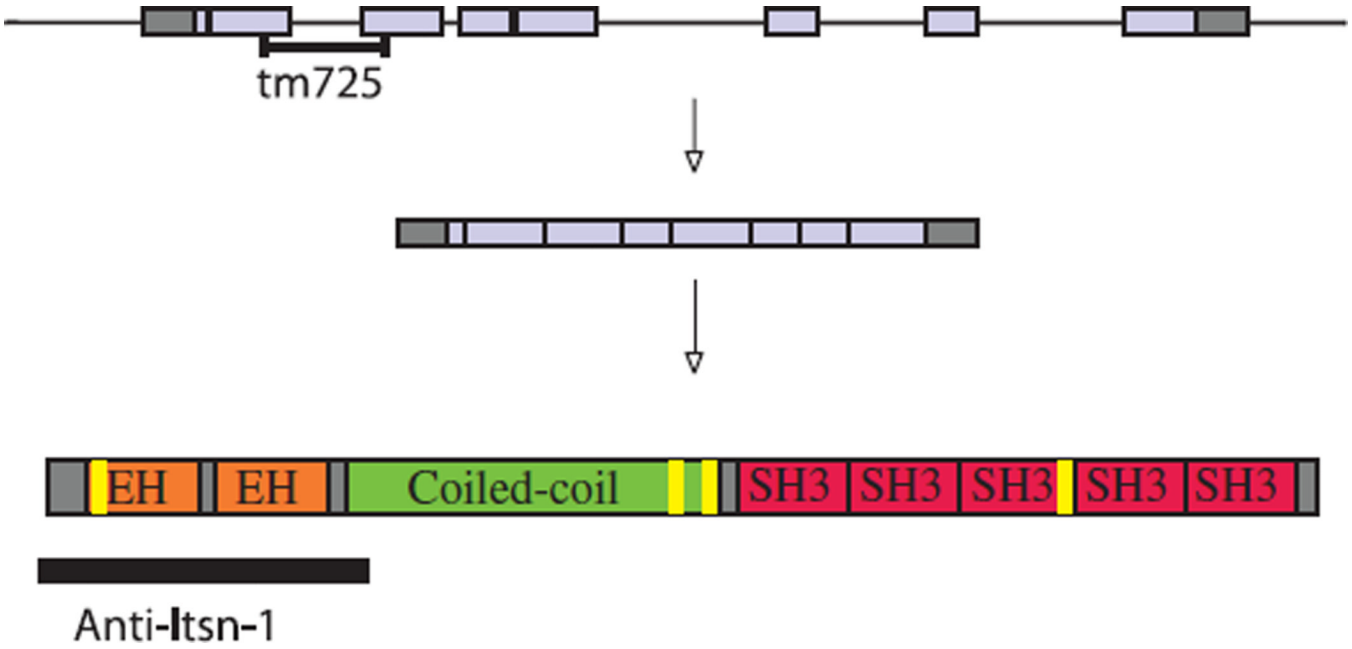

Figure 1. *C. elegans* ITSN-1 in wild-type and *itsn-1* deletion mutants

Schematic structure of *itsn-1* gene and its protein product. There are eight exons coding for a 1085 amino acid protein consists of two N-terminal EH domains, a center coiled-coil domain, five C-terminal SH3 domains and predicted α-adaptin interaction motifs (in yellow). The genomic region deleted in *itsn-1 (tm725)* mutants is as indicated. An N-terminal fragment of ITSN-1 was fused to GST and used as antigen to generate rabbit anti-ITSN-1 antibodies.

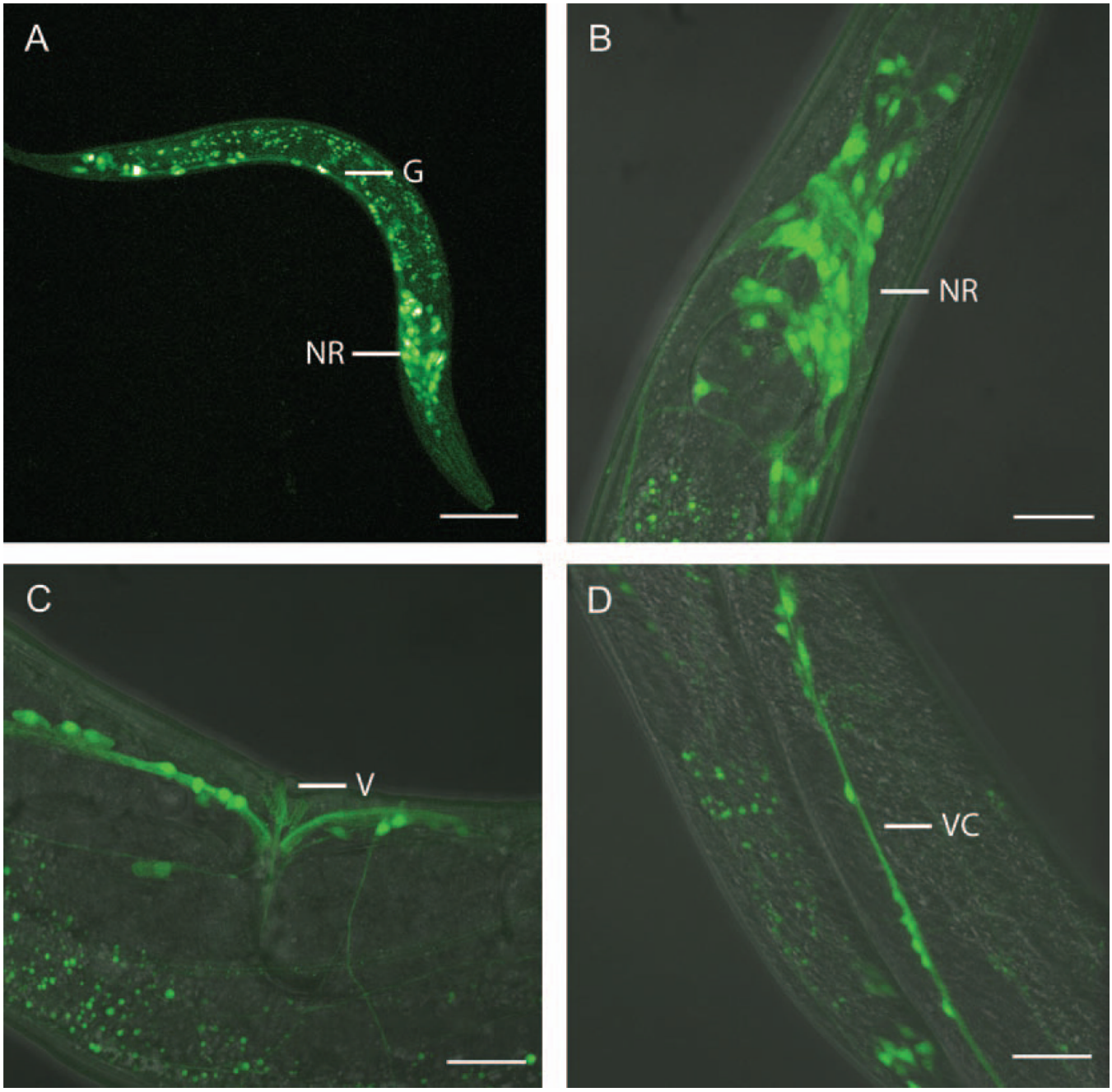

Figure 2. *Pitsn-1-GFP* is expressed in the nervous system

A–D) Animals carrying an *itsn-1* promoter-driven GFP reporter display predominant expression in the nervous system. L1 larva lateral view with head down (A), adult lateral view with head up shows pharyngeal motor neurons and intereeurons (B), adult lateral view shows ventral cord motor neurons along the vulva area (C), adult ventral view with tail up shows ventral cord motor neurons (D). NR (nerve ring), VC (ventral nerve cord), V (vulva), G (gut – autoflorescence). Scale bars in panels A–D correspond to 20 μm.

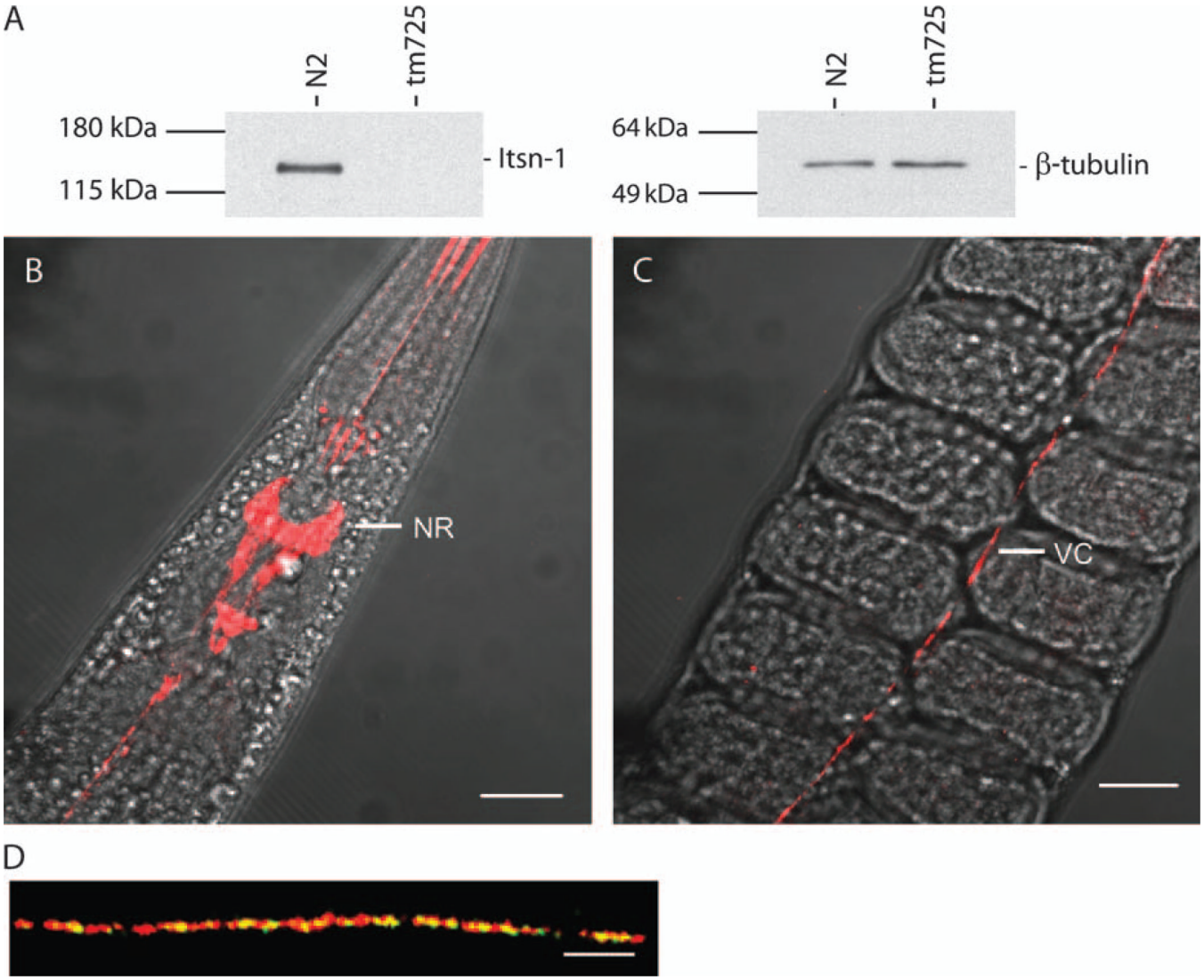

Figure 3. ITSN-1 protein is expressed in the nervous system and localized to synaptic vesicle enriched regions at the NMJ

A) Western blot analysis using affinity-purified anti-ITSN-1 antibodies shows the presence of ITSN-1 protein in wild-type (N2) but not in *tm725 itsn-1* null mutant lysates. Monoclonal antibody E7, which recognizes *C. elegans* β-tubulin, was used as a loading control. B,C). Whole-mount immunostaining of wild-type (N2) animals with the same anti-ITSN-1 antibodies. NR, nerve ring; VC, ventral nerve cord. D) GFP: :ITSN-1 signals colocalizes to synaptic vesicles. Shown in this panel is the dorsal nerve cord puncta with head of the animal to the left. GFP: :ITSN-1 puncta (green) show substantial colocalization with the synaptic vesicle marker SNT-1 (red). Scale bars in panels (B) and (C) correspond to 20 μm and in panel (D) to 5 μm.

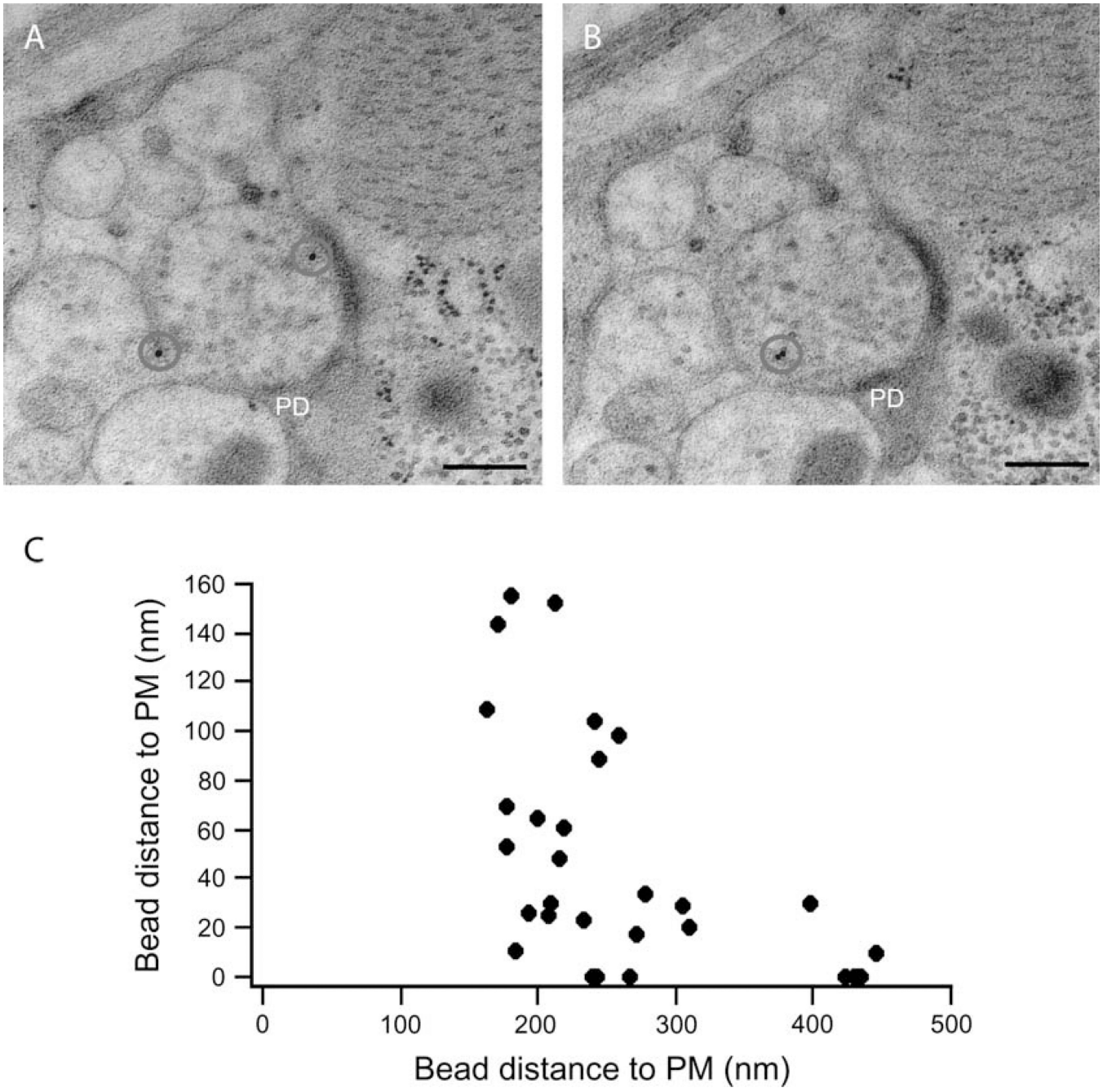

Figure 4. ITSN-1 is localized to endocytic hotspots in the NMJ

Immunoelectron microscopy analysis of ITSN-1 protein in wild-type animals. Endogenous ITSN-1 localization within the NMJ (A) and (B). The most densely labeled areas were associated with vesicles 200–300 nm from the PD (A B and C). Note, for both panels A and B, membranes are poorly defined under fixation conditions (required for immunoelectron microscopy), but can be seen at higher magnification. The scale bar represents 200 nm. PD (presynaptic density), PM (plasma membrane).

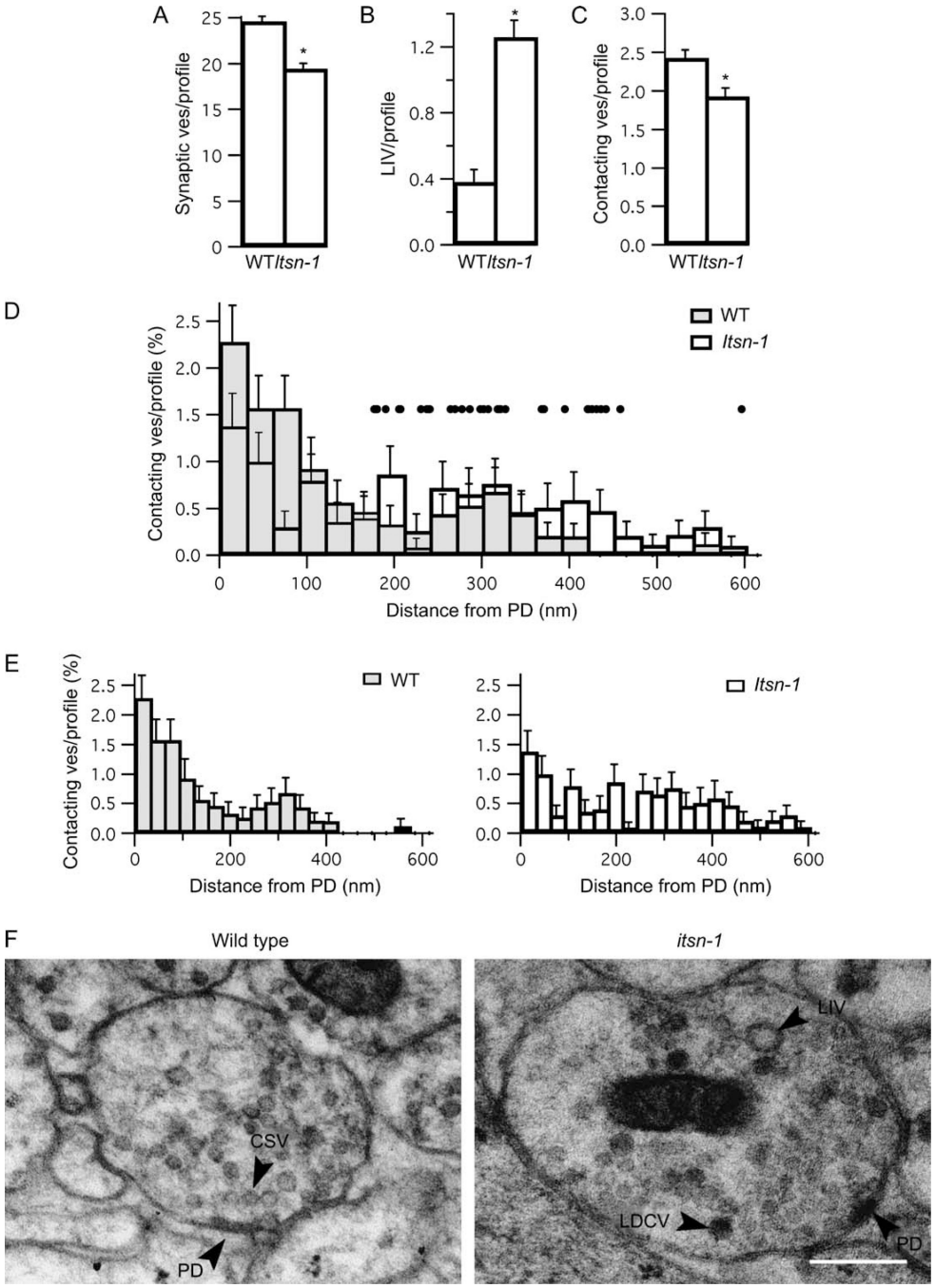

Figure 5. *itsn-1* mutants exhibit altered synaptic ultrastructure consistent with endocytic defects

The synaptic profiles from wild-type and *itsn-1 (tm725)* mutant NMJs were compared for A) total vesicle number, B) number of LIV and C) number of plasma membrane contacting vesicles. D) The distance of plasma membrane contacting vesicles relative to the PD, expressed as a ratio of total vesicles per profile for wild-type shaded bars and itsn-1 mutants clear bars (bar graphs are separated for clarity in panel E). Superimposed dots in panel (D) represent the distribution of ITSN-1 protein in wild-type synapses that is associated with, or within 30 nm of, the plasma membrane (ITSN-1 protein detected using anti-ITSN-1 primary and gold-labeled secondary antibodies as in Figure 4). (F) Representative synaptic profiles of wild-type and *itsn-1 (tm725)* mutant NMJs. Arrow heads indicate examples of an LIV,

clear synaptic vesicle (CSV), large dense core vesicle (LDCV) and the PD. The scale bar represents 200 nm.

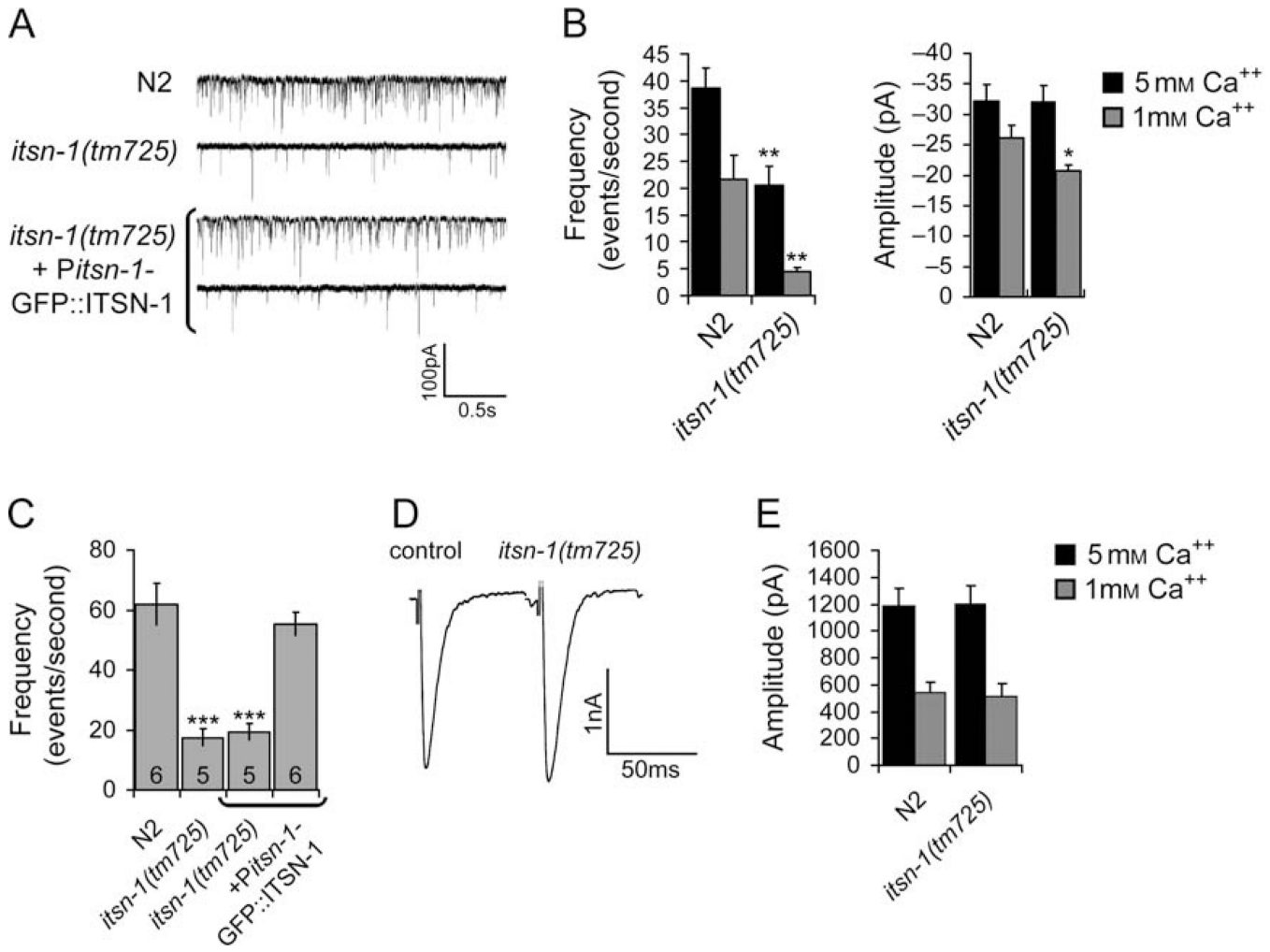

Figure 6. The *itsn-1(tm725)* mutant shows defective endogenous synaptic activity

A) Representative traces of mPSC events for wild-type (N2) (controls, upper trace), *itsn-1 (tm725)* mutant (second trace from the top) and *itsn-1 (tm725)* mutants carrying the *Pitsn-1*-GFP: :ITSN-1 rescuing construct (lower traces), recorded in voltage-clamp mode in 5 mM extracellular calcium. B) Averaged miniature event frequency (left graph) and amplitude (right graph) at 5 mM (black) and 1 mM (grey) extracellular calcium for controls and *tm725* transgenic and nontransgenic animals (all groups $n = 10$ except *tm725*1 mM Ca^{++} $n = 8$). C) The defect in mPSCs frequency can be rescued to wild-type levels by expressing the *Pifsn-1*-GFP: :ITSN-1 construct. Genotypes are as indicated with approximately half of the *itsn-1(tm725)* mutants that carry the P/fsn-7-GFP: :ITSN-1 construct showed a complete rescue of mPSC frequency. The number of recordings is indicated for each group. D) Representative responses evoked by electrical stimulation of the ventral nerve cord for wild-type (N2) and *itsn-1(tm725)* mutant animals. E) The averaged evoked response amplitude was not affected by the *tm725* mutation (Controls $n = 10$, *itsn-1(tm725),* $n = 11$ and $n = 5$ at 5 and 1 mM Ca^{++}, respectively). Data represent mean ± SEM. *$p < 0.05$, **$p < 0.01$ and ***$p < 0.001$.

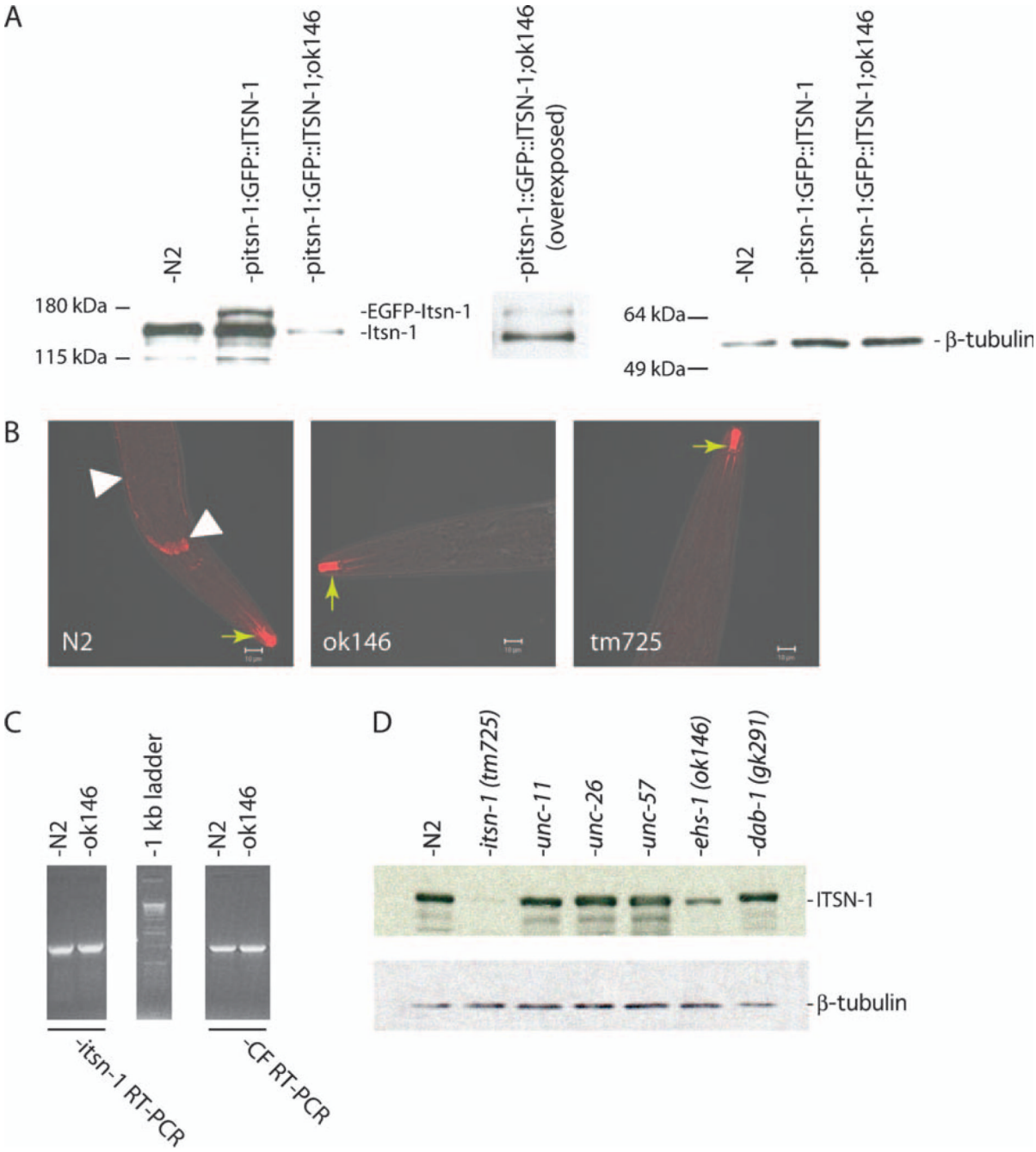

Figure 7. EHS-1 is required for ITSN-1 protein accumulation *in vivo*

A) Immunoblot of wild-type (N2), GFP: :ITSN-1 transgenic animals expressing an N-terminally GFP-tagged ITSN-1 on N2 genetic background, or on an *ehs-1 (ok146)* null mutant background (*Pitsn-1:* GFP;*ok146*) stained with rabbit anti-ITSN-1 polyclonal antibody. β-tubulin was used as the loading control. B) ITSN-1 staining in wild-type N2, *ehs-1 (ok146)* and negative control *itsn-1 (tm725)* mutants. Specific staining in the nervous system was detected in wild-type animals but not in *ok146or tm725* mutants (white arrowheads). Non-specific staining was observed in the mouth of each animal, regardless of genotype (yellow arrows). Scale bars represent 10 μm.C) Semiquantitative RT-PCR analysis of *itsn-1* gene expression in wild-type N2 and *ehs-1 (ok146)* mutant animals show that

decreased levels of ITSN-1 protein accumulation in *ok146* is not associated with a reduction in *itsn-1* mRNA expression. RT-PCR assays were standardized using RT-PCR to detect *C. elegans* eukaryotic initiation factor 4A (CelF) gene expression as a control. D) Western blot analysis with ITSN-1 antibody probed against total protein lysates from wild-type animals (N2) and endocytic mutants.

Table 1

The itsn-1 genetic interaction screen

EH domain proteins
Itsn-1 (ok268);ehs-1 (ok146) – Eps15
Itsn-1 (tm725);ehs-1 (ok146)
Itsn-1 (ok268);rme-1 (b1045) – Ehd
Itsn-1 (tm725);rme-1 (b1045)
itsn-1 (tm725);Y39B6A.38(tm2156) – Reps-1
SH3 domain proteins
Itsn-1 (tm725);sem-5(cs15) – Grb2
Itsn-1 (ok268);nck-1 (ok694) – Nck2
Itsn-1 (ok268);pqn-19(ok406) – Stam-1
itsn-1 (tm725);K08E3.4(ok925) – Drebin-like protein
Itsn-1 (tm725);tag-218(ok494) – ephexin
Itsn-1 (tm725);unc-57(ok310) – endophilin
Itsn-1 (ok268);B0336.6(ok640) – Abi1/e3B1
Endocytosis and selected other structural and signaling proteins
Itsn-1 (ok268);dyn-1 (ky51) – dynamin
Itsn-1 (tm725);dyn-1(ky51)
Itsn-1 (ok268);wsp-1 (gm324) – Wasp
Itsn-1 (tm725);wsp-1 (gm324)
Itsn-1 (tm725);unc-11(e47)–AP 180
Itsn-1 (tm725);unc-26(m2) – synatojanin
Itsn-1 (ok268);alx-1 (gk275) – Alixl
Itsn-1 (ok268);sli-1(sy143) – Cbl-b
Itsn-1 (tm725);dnc-1 (or404) – dynactin
Itsn-1 (ok268);syd-2(ju37) α–liprin
Itsn-1 (tm725);gei-18(ok788)
Itsn-1 (ok268);rpm-1 (ju41) – PAM/highwire
itsn-1 (tm268);dab-1 (gk291) – Disabled2 *
Itsn-1 (tm725);dab-1(gk291) *
Receptors
itsn-1 (ok268);let-23(sa62)-EGFR-unc-4(e120)/mnC1 Dpy-10(e128)unc-52(e44)
Itsn-1 (ok268);vab-1 (d×31) – EphB
Itsn-1 (ok268);vab-1 (e699)
itsn-1 (tm725);unc-29(e1072) – AchR subunit
itsn-1 (tm725);unc-49(e407) – GABAR subunit
Ehs-1 test
ehs-1(ok146);dab-1(gk291) *

Various double mutants with *itsn-1 (and ehs-1)* were generated and tested for evidence of a synthetic sick or lethal phenotype, as well as for synthetic locomotory defects. Although qualitative enhancement or suppression of phenotypes that had been previously defined in single mutant animals was not observed, we did not quantify such phenotypes.

* L1 L4 larval arrest with severe and progressive paralysis leading to the lethality.